PHYSICAL REVIEW E

STATISTICAL PHYSICS, PLASMAS, FLUIDS, AND RELATED INTERDISCIPLINARY TOPICS

THIRD SERIES, VOLUME 62, NUMBER 3 PART B SEPTEMBER 2000

ARTICLES

Deuteron NMR study of molecular dynamics in a compound exhibiting a reentrant nematic phase

R. Y. Dong,[1] A. Carvalho,[2] P. J. Sebastião,[2] and H. T. Nguyen[3]

[1]*Department of Physics and Astronomy, Brandon University, Brandon, Manitoba, Canada R7A 6A9*

[2]*Centro de Física da Matéria Condensada, Avenida Prof. Gama Pinto 2, 1649-003 Lisboa Codex, Portugal and Instituto Superior Técnico, Departamento de Física, Avenida Rovisco Pais, 1049-001 Lisboa Codex, Portugal*

[3]*CNRS, Centre de Recherche Paul Pascal, Avenue A. Schweitzer, and F-33600 Pessac, France*

(Received 27 March 2000)

A deuteron NMR study of molecular dynamics in the partial bilayer smectic A_d and reentrant nematic phases of a pure chain-deuterated compound is presented. The deuteron spin-lattice relaxation times T_{1Z} and T_{1Q} were measured as a function of temperature for two different frequencies (15 and 46 MHz). The experimental results were interpreted in terms of the internal conformational motions of a chain decoupled from the molecular small-step rotational diffusion and the order director fluctuations. The latter motion was found to be essential to the fit of experimental results in the reentrant nematic phase. The fitting parameters obtained by using a global target fitting method are acceptable when compared with those obtained from other deuteron and proton NMR studies of the same mesophases.

PACS number(s): 61.30.−v

I. INTRODUCTION

NMR spectroscopy is a very powerful technique in the study of liquid crystals [1]. Both proton and deuteron NMR studies were carried out in liquid crystals in order to better understand the molecular order and dynamics in these materials, in particular in the nematic and smectic-*A* mesophases [2–14]. Valuable information on the dynamical processes in these compounds such as molecular reorientations (MR's), internal rotations (IR's), translational self-diffusion (SD), and collective motions known as order director fluctuations (ODF's) can be obtained with these techniques. The results obtained from deuteron and proton studies can be complementary, since deuteron and proton NMR relaxations can be sensitive to different types of motions.

The proton NMR spin-lattice relaxation time T_{1Z} is sensitive to all types of movements, but due to dipolar interactions it is not possible to separate internal motions from the overall molecular reorientations. However, these studies can cover a very broad frequency range (500 Hz to 500 MHz) when combining standard and fast field cycling NMR techniques [13,15,16]. Due to the large frequency range, it is usually possible to separate the ODF from SD and MR relaxation mechanisms. On the other hand, deuteron NMR is site specific, and by means of multipulse techniques two different deuteron spin-lattice relaxations times, T_{1Z} (Zeeman) and T_{1Q} (quadrupolar), can be simultaneously determined at various atomic sites. The extraction of the spectral densities $J_1(\omega_0)$ and $J_2(2\omega_0)$, where ω_0 is the Larmor frequency, can then be carried out. Indeed, an IR relaxation mechanism in the side chain(s) of a flexible mesogen can best be studied by deuterons as a probe, when the internal conformational changes in the molecules may be assumed to decouple from molecular reorientations [1]. A deuteron NMR study of a chain-deuterated 4-*n*-octyloxy-4′-cyanobiphenyl (8OCB) [17] which demonstrates the ability to study molecules with an increasing number of conformational transitions, was recently reported. However, the nuclear quadrupolar interaction of the deuteron's spin ($I=1$) is dominant, which makes the spin-lattice relaxation mainly sensitive to intramolecular relaxation mechanisms. Therefore, only in a very indirect way is it possible to include the influence of the translational motions of the molecules. The deuteron measurements are usually made at frequencies above 10 MHz, where the contribution of the collective motions is negligible in the smectic-*A* phases [13,18], but can be as much as 30% of the overall relaxation rate in the nematic mesophases [13,14,18,19] when compared with molecular reorientations. As the proton studies show [13,18] that, above 10 MHz, the ODF mechanism can be masked by both the MR and SD

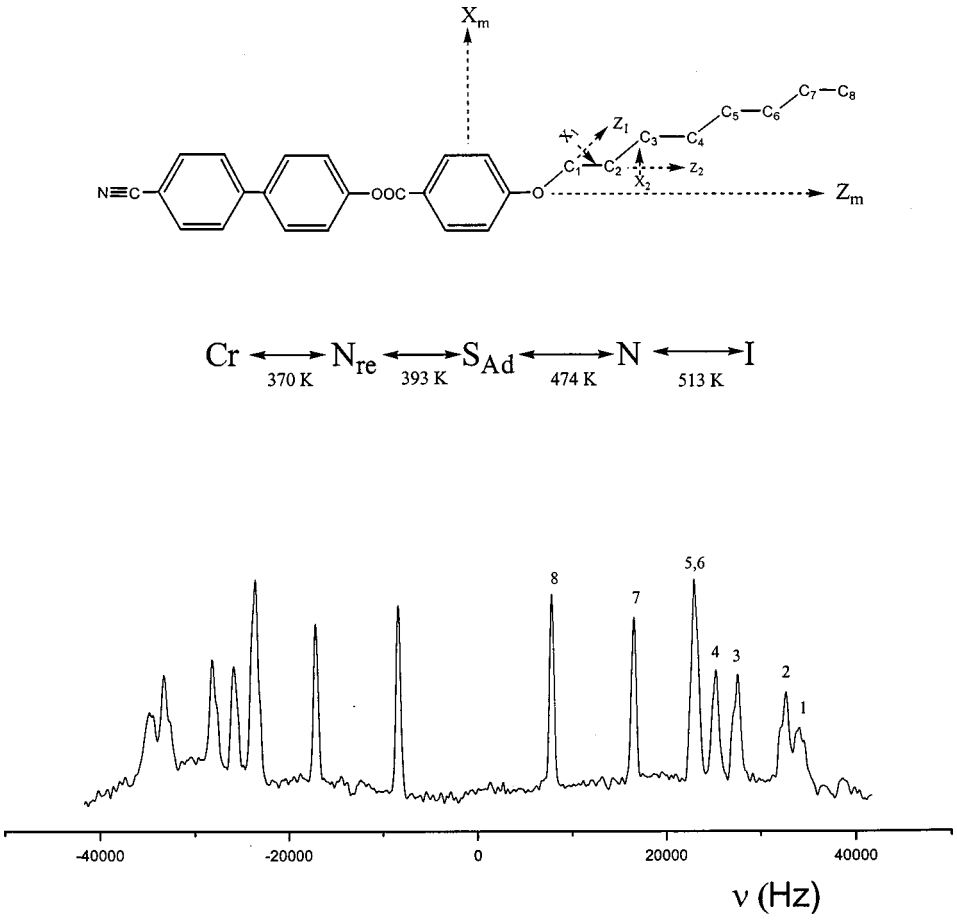

FIG. 1. A typical deuteron NMR spectrum of 8OBCB-d_{17} showing the peak assignment, together with a 8OBCB molecule showing the various coordinate systems used in the text.

relaxation mechanisms, deuteron studies can be very helpful since they are insensitive (in a first approximation) to SD's. Nevertheless, the small contribution of ODF's at the selected frequencies and the high correlation between the strength factor A and the high frequency cutoff of ODF's [20–23] have made it difficult to separate their importance to the relaxation model.

Previous studies of the molecular dynamics in the reentrant nematic (N_{re}) phases of pure compounds [13,24] and mixtures of compounds [10,14,25,26] with strong polar cyano end groups, revealed that the molecular dynamics in these phases is not remarkably different from the one observed for the nonreentrant ones. However, the exact importance of ODF's to the relaxation rate remains an open question. In the present study, we follow the methodology used for 8OCB to examine this important question in a high clearing temperature compound octyloxy benzoyloxy cyanobiphenyl [27,28] (see 8OBCB in Fig. 1) which exhibits a nematic (N) phase, a smectic-A_d phase, and an N_{re} phase. The experimental spectral densities determined by deuterium NMR were interpreted in terms of a relaxation model which decouples the small-step rotational diffusion of the molecules [29–34] from the internal conformational motions of the chain [35–37]. The internal motions in the octyloxy chain were treated using the rotameric state model of Flory [38]. As in 8OCB, the pentane effect, which assumes an infinitely large energy in forming a g^+g^- or g^-g^+ linkage in the carbon-carbon chain, is used to reduce the number of configurations to 577. The experimental results for the low temperature N_{re} phase were analyzed using a global target minimization approach in order to obtain more reliable fitting parameters [13,14,17,39]. In this phase, order director fluctuations were also considered. Owing to the limitation of the temperature range in our spectrometers, we were unable to collect data in the smectic-A_d phase at both frequencies to warrant a detailed analysis. The paper is organized as follows: Sec. II presents the necessary formulas for the interpretation of our data, Sec. III outlines the experimental method, and Sec. IV describes the results and discussion.

II. BASIC THEORY

The complete description of the formulas necessary to discuss our experimental splitting and spectral density data can be found in the literature [1,17]. The additive potential (AP) method [40] is used to model the quadrupolar splittings along the octyloxy chain. The O—C_1 bond in 8OBCB is taken to be fixed on the phenyl ring plane with a C_{ar}—O—C_1 angle of 126.4° [41]. The C—C—C, C—C—H, and H—C—H angles are assumed [42] to be 113.5°, 107.5°, and 113.6°, respectively. The O—C bond is taken to be identical to a C—C bond, and the O—C—C angle is set the same as a C—C—C angle. The dihedral angles ($\phi = 0, \pm 112°$) are for rotation about each C—C bond, and also about the O—C bond in the octyloxy chain. The segmental order parameter of the C—D bond ($S_{CD}^{(i)}$) at the ith carbon site is directly related to the quadrupolar splitting $\Delta\nu_i$ according to the relation

$$\Delta\nu_i=\frac{3}{2}q_{CD}^{(i)}S_{CD}^{(i)}, \tag{1}$$

where $q_{CD}=e^2qQ/h$, the quadrupolar coupling constant, is 165 kHz for the methylene deuterons. By modeling the segmental order profile at each temperature, the interaction parameters for the molecular core X_a and for a C—C bond X_{cc} used to parametrize the potential of mean torque $U_{ext}(n,\Omega)$ [40] can be determined. Simultaneously the order parameter tensor for an ''average'' conformer of the molecule can also be evaluated [1].

The evolution of a spin system is governed by a spin Hamiltonian which contains time fluctuating terms as a result of thermal motions of the liquid-crystal molecules. From the standard spin relaxation theory for deuterons [43], the Zeeman and quadrupolar spin-lattice relaxation rates are given by

$$\begin{aligned} T_{1Z}^{-1}&=J_1(\omega_0)+4J_2(2\omega_0),\\ T_{1Q}^{-1}&=3J_1(\omega_0), \end{aligned} \tag{2}$$

where the spectral densities are given by

$$J_m(m\omega)=\frac{3\pi^2}{2}(q_{CD})^2\int_0^\infty G_m(t)\cos(m\omega t)dt, \tag{3}$$

with the time-autocorrelation functions

$$G_m(t)=\langle D_{m0}^2(\Omega_{LQ}(0))D_{m0}^{2*}(\Omega_{LQ}(t))\rangle \tag{4}$$

given in terms of the Wigner rotation matrix $D_{mn}^2(\Omega)$ in the fluctuating spin Hamiltonian, the angular brackets denote an ensemble average, and the Euler angles $\Omega_{LQ}(t)$ specify the orientation of the principal axes of the electric-field-gradient tensor with respect to the laboratory frame whose z_L axis is defined by the external magnetic field. Now different motional processes like IR's, MR's, and ODF's can influence the spin Hamiltonian. These motional processes occur over sufficiently different time scales such that small couplings among them can often be neglected. For flexible molecules forming uniaxial mesophases, the orienting potential needed in solving the rotational diffusion problem is first established from the order tensor of an ''average'' conformer. For the deuterons in the chain, the decoupled model [36,37] is used to describe correlated internal rotations in the octyloxy chain, and an extension of the Nordio model is used [29] to account for rotational diffusions of the molecule. Hence, the spectral densities $J_{mR}^{(i)}(m\omega)$ for the deuterons on the C_i carbon of the chain for $m\neq 0$ are given in the notation of Ref. [29] by

$$\begin{aligned} J_{mR}^{(i)}(m\omega)=\frac{3\pi^2}{2}(q_{CD}^{(i)})^2\sum_n\sum_{n'}\sum_{k=1}^{577}&\left(\sum_{l=1}^{577}d_{n,0}^2(\beta_{M,Q}^{(i)l})\right.\\ &\left.\times\exp[-in\alpha_{M,Q}^{(i)l}]x_l^{(1)}x_l^{(k)}\right)\left(\sum_{l'=1}^{577}d_{n',0}^2(\beta_{M,Q}^{(i)l'})\right.\\ &\left.\times\exp[-in'\alpha_{M,Q}^{(i)l'}]x_{l'}^{(1)}x_{l'}^{(k)}\right)\\ &\times\sum_j\frac{(\beta_{mnn'}^2)_j[(\alpha_{mnn'}^2)_j+|\lambda_k|]}{m^2\omega^2+[(\alpha_{mnn'}^2)_j+|\lambda_k|]^2} \end{aligned} \tag{5}$$

where $\beta_{M,Q}^{(i)l}$ and $\alpha_{M,Q}^{(i)l}$ are the two polar angles for the C_i—D bond of the conformer l in the molecular frame (Fig. 1) attached to the molecular core, λ_k and $\vec{x}^{(k)}$ are the eigenvalues and eigenvectors from diagonalizing a symmetrized transition rate matrix, and $(\alpha_{mnn'}^2)_j/D_\perp$ (the decay constants) and $(\beta_{mnn'}^2)_j$ [the relative weights of the exponentials in $G_m(t)$] are the eigenvalues and eigenvectors from diagonalizing the matrix of the rotational diffusion operator [29]. The rate matrix describing conformational changes in the octyloxy chain contains jump constants k_1, k_2, and k_3 for one-, two-, and three-bond motions [37,44] in the chain. The rate matrix is not symmetrical, owing to the fact that transitions among two possible conformations via one of elementary jump constants are weighed differently by their equilibrium probabilities $P_{eq}(n)$.

The effect of chain flexibility on the ODF contribution to the spectral density was discussed previously in Ref. [19]. When considering ODF's to second order, for the C_i deuterons one obtains

$$J_{1DF}^{(i)}(\omega)=\frac{3\pi^2}{2}(q_{CD}^{(i)})^2\frac{A(1-4\alpha)}{(1-3\alpha)^2}(S_{CD}^{(i)})^2\Im(\omega_c/\omega)/\sqrt{\omega}, \tag{6}$$

where $\Im(\omega_c/\omega)$ is the cutoff function [45] with ω_c being the high frequency cutoff, A is the standard prefactor which depends on viscoelastic parameters of the sample, α is a parameter related to A which gives a measure of the magnitude of ODF's, and a much smaller contribution

$$\begin{aligned} J_{2DF}^{(i)}(2\omega)=\frac{3\pi^2}{2}(q_{CD}^{(i)})^2\frac{A^2}{(1-3\alpha)^2}(S_{CD}^{(i)})^2\frac{1}{3\pi}\\ \times\ln[1+(\omega_c/2\omega)^2]. \end{aligned} \tag{7}$$

The factor $(1-4\alpha)$ in Eq. (6) is needed to account for the second order ODF contribution [46]. The calculated spectral densities for the C_i deuterons are now given by

$$J_1^{(i)}(\omega)=J_{1R}^{(i)}(\omega)+J_{1DF}^{(i)}(\omega), \tag{8}$$

$$J_2^{(i)}(2\omega)=J_{2R}^{(i)}(2\omega)+J_{2DF}^{(i)}(2\omega) \tag{9}$$

under the above mentioned assumptions.

III. EXPERIMENTAL METHOD

A home-built superheterodyne coherent pulse NMR spectrometer was operated for deuterons at 15.1 MHz using a Varian 15-in. electromagnet, and at 46.05 MHz using a 7.1-T Oxford superconducting magnet. The temperature gradient across the sample in the NMR probe was estimated to be better than 0.3 °C. The $\pi/2$ pulse width is about 4 μs. Pulse control and signal collection were performed by a GE 1280 minicomputer. A broadband Wimperis sequence [47] was used to simultaneously measure the T_{1Z} and T_{1Q} spin-lattice relaxation times. Signal collection was started 10 μs after each monitoring $\pi/4$ pulse, and averaged over 96–160 scans at 46 MHz and up to 640 scans at 15.1 MHz depending on the signal strengths. A description of data reductions was

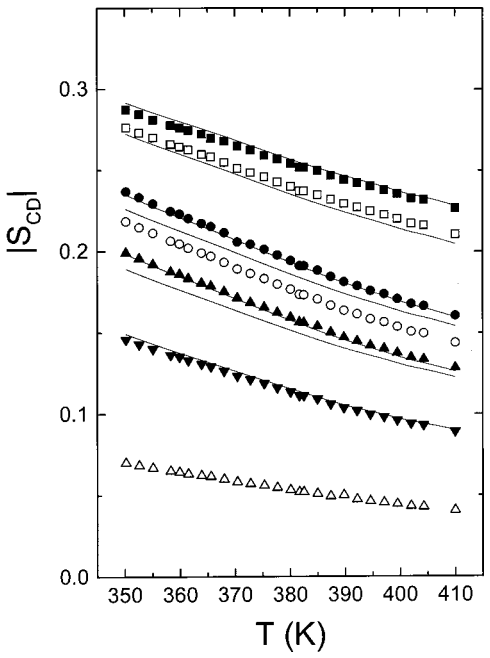

FIG. 2. Plot of segmental order parameters vs the temperature. Solid squares, circles, up-triangles, and down-triangles denote C_1, C_3, $C_{5,6}$, and C_7 sites, respectively. Open squares, circles, and up-triangles denote C_2, C_4, and C_8 sites, respectively. The solid curves are the theoretical calculations for C_1 to C_7 starting from the top.

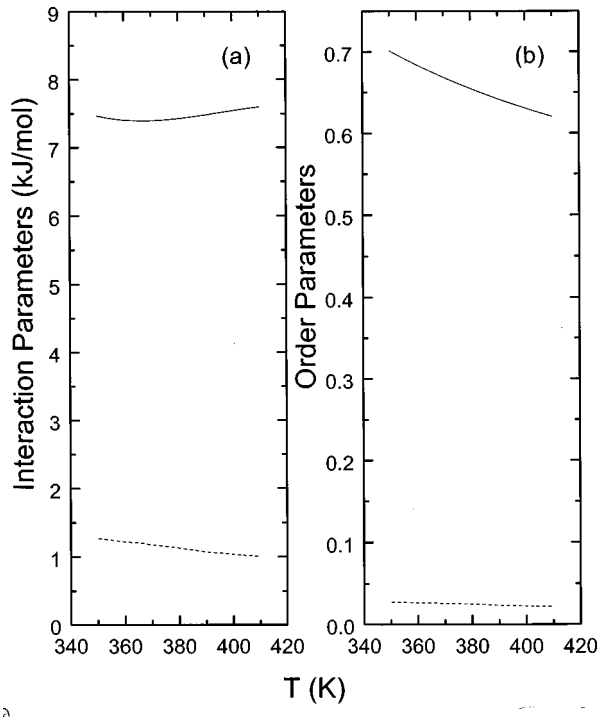

FIG. 3. (a) Plot of interaction parameters X_a (solid line) and X_{cc} (dashed line) vs the temperature. (b) Plots of the order parameters $\langle P_2 \rangle$ (solid line) and $\langle S_{xx}\text{-}S_{yy} \rangle$ (dashed line) of an ''average'' conformer of 8OBCB as a function of temperature.

previously given [48]. The experimental accuracy in measuring the relaxation times is estimated to be about 5%.

Due to its high clearing temperature and the temperature limitations in our NMR probes, the chain-deuterated 8OBCB-d_{17} sample was not heated to the isotropic phase for aligning the director. Fortunately we were able to achieve the alignment of the director along the external magnetic field in the N_{re} phase. The peak assignment of a representative spectrum of 8OBCB-d_{17} is also shown in Fig. 1. The splittings assigned to various deuterons on different carbon sites are assumed to decrease monotonically from the core down the octyloxy chain, with the exception of deuterons on the carbons 5 and 6 which present similar splittings, as can be inferred from the line intensity [28]. This seems to be consistent with our measured spin-lattice relaxation times at these carbon sites, as well as our modeling of segmental order parameters. Due to the lack of specifically site-deuterated compounds, we have no reason to reverse splittings at carbon 3 and 4, as was assumed in 8OCB [17].

IV. RESULTS AND DISCUSSION

Figure 2 shows the experimental segmental order parameter $S_{CD}^{(i)}$ as a function of temperature in the N_{re} and S_{Ad} phases of 8OBCB-d_{17}. An optimization routine (AMOEBA) [49] was used to minimize the sum squared error f in fitting the experimental $S_{CD}^{(i)}$,

$$f = \sum_i \left(|S_{CD}^{(i)}| - |S_{CD}^{(i)Calc}| \right)^2, \tag{10}$$

where the sum over i includes only the methylene deuterons in C_1 to C_7. The f values at different temperatures are of the order of 10^{-3}. We have not included the methyl splitting in our minimization, since it has been known to be sensitive to the assumed value of the C—C—H angle of the methyl group. Furthermore, the relaxation of the methyl group was not considered due to possible complication from methyl rotations about its threefold axis. In the AP method, we set E_{tg}(C—C—C)=3500 J/mol and E_{tg}(O—C—C)=4900 J/mol. These E_{tg} values are slightly lower than those used in 8OCB. The calculated segmental order parameters are indicated in Fig. 2 as solid lines. The derived interaction parameters X_a and X_{cc} are plotted versus the temperature in Fig. 3(a). We found that these values are comparable to those found in other cyanobiphenyl compounds [14,17]. It is interesting, however, to note that X_a is nearly temperature insensitive, in contrast with that found for 8OCB. This may be due to the N_{re} phase being below a more ordered smectic-A_d phase. The interaction parameters found from fitting the quadrupolar splittings are used to find the equilibrium probability $P_{eq}(n)$ of conformer n. Furthermore, the order matrix of an ''average'' conformer of 8OBCB has been evaluated at each temperature. Figure 3(b) shows its principal elements $\langle P_2 \rangle$ and $\langle S_{xx} - S_{yy} \rangle$ as functions of temperature. While $\langle P_2 \rangle$ varies from 0.66 to 0.38 upon approaching the isotropic phase in 8OCB, it changes only from 0.7 to 0.62 upon entering the smectic-S_d phase in 8OBCB. Despite some obvious deviations between calculated and observed segmental order parameters in Fig. 2, in particular $S_{CD}^{(4)}$ and $S_{CD}^{(6)}$, the derived $P_{eq}(n)$ and the potential of mean torque are quite satisfactory for treating our relaxation data below.

The spectral density $J_1(\omega)$ and $J_2(2\omega)$ data at 15.1 and

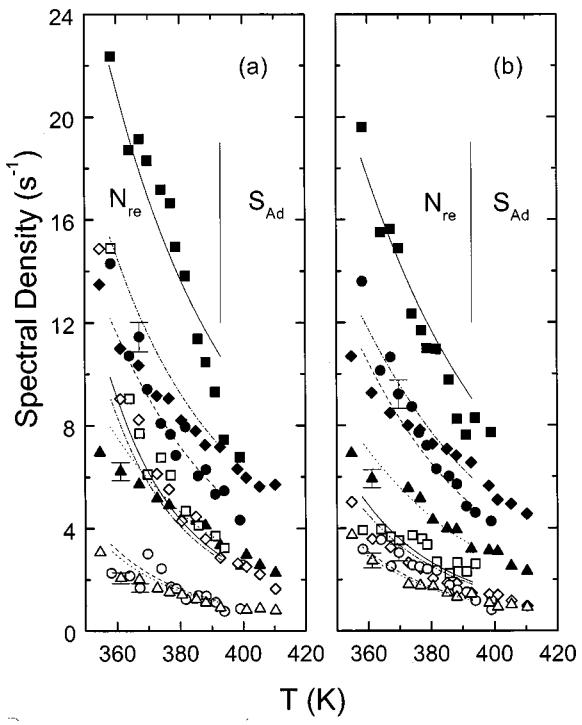

FIG. 4. Plots of spectral densities vs temperature in 8OBCB. Closed symbols denote $J_1^{(i)}(\omega)$, and open symbols denote their corresponding $J_2^{(i)}(2\omega)$. (a) Squares and circles are for C_1 and C_3 at 15.1 MHz, while diamonds and triangles are for C_1 and C_3 at 46 MHz. Solid and dashed curves denote calculated J_1 and J_2 for C_1 and C_3 at 15.1 MHz, while dot-dashed and dotted curves for C_1 and C_3 at 46 MHz. (b) Squares and circles are for C_2 and C_4 at 15.1 MHz, while diamonds and triangles are for C_2 and C_4 at 46 MHz. Solid and dashed curves denote the calculated J_1 and J_2 for C_2 and C_4 at 15.1 MHz, and dot-dashed and dotted curves J_1 and J_2 for C_2 and C_4 at 46 MHz. Typical error bars are shown only for C_3 and C_4.

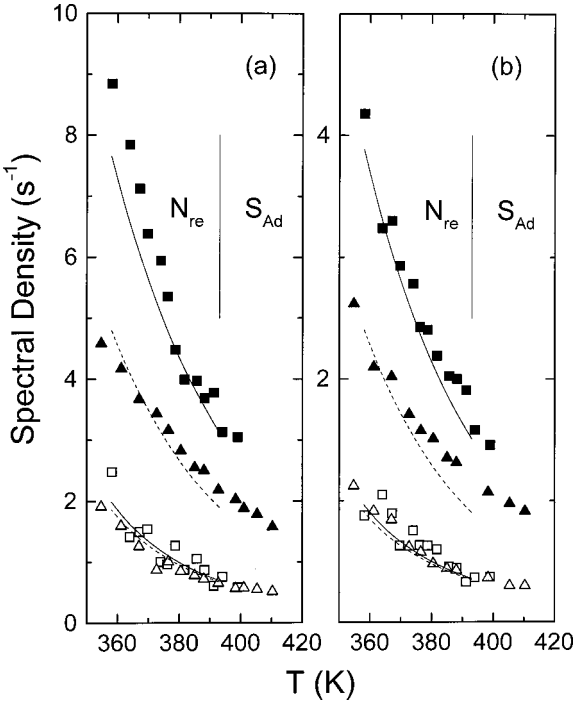

FIG. 5. Plots of spectral densities vs temperature in 8OBCB. Closed symbols denote $J_1^{(i)}(\omega)$, and open symbols denote their corresponding $J_2^{(i)}(2\omega)$. (a) Squares and triangles are for $C_{5,6}$ at 15.1 and 46 MHz, respectively. (b) Squares and triangles are for C_7 at 15.1 and 46 MHz, respectively. Solid and dashed curves are calculated spectral densities at 15.1 and 46 MHz, respectively.

46 MHz versus the temperature for all the methylene deuterons are shown in Figs. 4 and 5. It is clear from these figures that $J_1^{(i)}(\omega)$ shows substantial frequency dependences at all carbon sites, while $J_2^{(i)}(2\omega)$ shows little or no frequency dependences. The latter seems to differ from 8OCB as the frequency dependences of $J_2^{(i)}(2\omega)$ in 8OCB are a bit more pronounced [17]. As mentioned above, we will concentrate only on the spectral density data in the N_{re} phase. As in the N phase of 8OCB, some ODF contributions appear to be necessary in the N_{re} phase of 8OBCB. As collective motions are slow and only effective in relaxing nuclear spin at low frequencies (below 1 MHz in most cases), we have chosen A and the high frequency cutoff by trial and error such that the ODF contribution in Eq. (8) amounts to about 35% of the total at 15.1 MHz. We have also assumed that the prefactor A is constant in the N_{re} phase, while imposing a linear temperature dependence for the high frequency cutoff ($\omega_c/2\pi = 35$ MHz at 363 K, and decreases to 25 MHz at the N_{re}-S_{Ad} phase transition at 393 K). This is consistent with the fact that the cutoff function $\mathfrak{I}(x)$ approaches zero in S_{Ad} phases at our Larmor frequencies. We found that the second order ODF contributions to $J_2^{(i)}(\omega)$ at 15.1 MHz are very small, while ODF's contribute to $J_1^{(1)}(\omega)$ between 33% (363 K) and 38% (393 K) at 15.1 MHz (about 10% for all temperatures at 46 MHz).

We believe that the motional biaxiality is small and have chosen $D_x = D_y = D_\perp$. The spectral densities $J_1^{(i)}(\omega)$ and $J_2^{(i)}(2\omega)$ for C_1 to C_7 are calculated using Eqs. (8) and (9), and compared with their experimental values in a global target analysis [39]. This approach takes advantage of the fact that the target model parameters vary smoothly with temperature. To get some idea about the temperature behaviors of model parameters $D_\perp$, $D_\parallel$, k_1, k_2 and k_3, individual target analyses (i.e., analyses of spectral densities at each temperature) were first carried out. We found that the rotational diffusion constants obeyed simple Arrhenius relations

$$D_\perp = D_\perp^\circ \exp[-E_a^{D_\perp}/RT], \tag{11}$$

$$D_\parallel = D_\parallel^\circ \exp[-E_a^{D_\parallel}/RT], \tag{12}$$

while the jump constants showed temperature behaviors which could be approximated by

$$k_i = k_i' + k_i''(T - T_{\max}), \tag{13}$$

where $i = 1$, 2 or 3, and $T_{\max}$ is 393 K in this study. The pre-exponentials $D_\perp^\circ$ and $D_\parallel^\circ$, and their corresponding activation energies $E_a^{D_\perp}$ and $E_a^{D_\parallel}$, are the global parameters. Similarly k_1', k_1'', k_2', k_2'', k_3', and k_3'', are the remaining global parameters in our global target analysis. Instead of Eqs. (11) and (12), these were rewritten in terms of the activation energies and the diffusion constants $D_\perp'$ and $D_\parallel'$ at $T_{\max}$. Indeed k_1', k_2', k_3', $D_\perp'$, and $D_\parallel'$ were first obtained at 393 K by an individual target analysis. The ODF prefactor A was inputed,

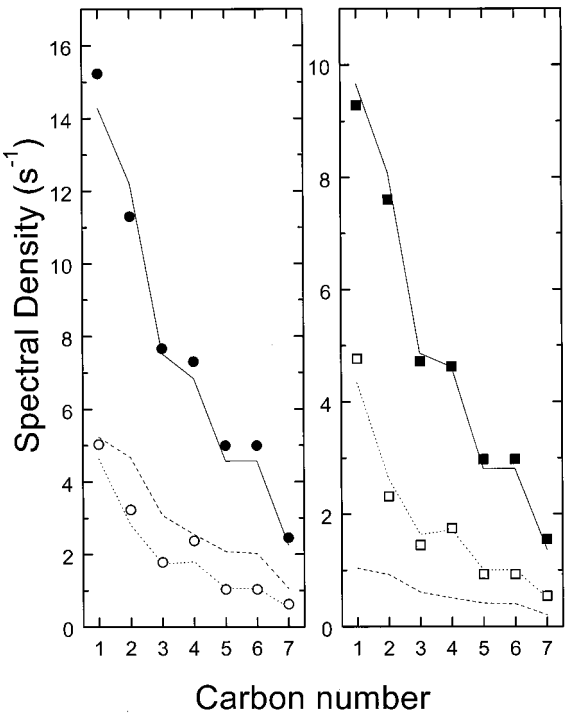

FIG. 6. Variation of the spectral densities $J_1(\omega)$ (solid symbols) and $J_2(2\omega)$ (open symbols) with the deuteron position in the reentrant nematic phase of 8OBCB ($T=378$ K). Circles and squares denote data from 15.1 and 46 MHz, respectively. Solid and dotted lines are predictions for J_1 and J_2, respectively, while dashed line denotes the theoretical $J_{1DF}^{(i)}(\omega)$.

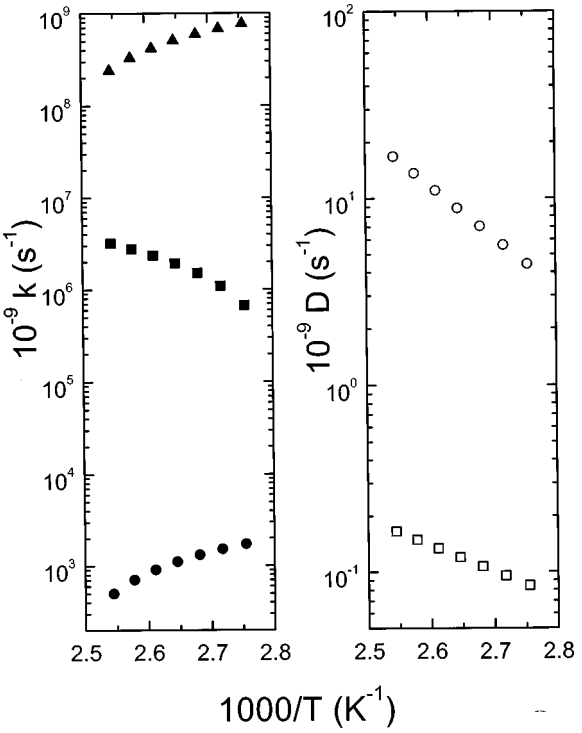

FIG. 7. Plots of jump rate constants k_1 (squares), k_2 (circles), and k_3 (triangles), as well as rotational diffusion constants $D_\parallel$ (circles) and $D_\perp$ (squares), as functions of the reciprocal temperature.

and found ''best'' at 4.7×10^{-6} s$^{1/2}$, a value consistent with those found in other liquid crystals [17,19]. Again AMOEBA [49] was used to minimize the mean-squared percent deviation (F). The fitting quality factor Q is defined as

$$Q=\frac{\sum_k\sum_\omega\sum_i\sum_m [J_m^{(i)calc}(m\omega)-J_m^{(i)exp\,t}(m\omega)]_k^2}{\sum_k\sum_\omega\sum_i\sum_m [J_m^{(i)exp\,t}(m\omega)]_k^2}, \tag{14}$$

where the sum over i covers C_1 to C_7, the sum over ω is for two different Larmor frequencies, the sum over k is for seven temperatures, and $m=1$ and 2. Since the signals from C_5 and C_6 deuterons overlapped, and their calculated spectral densities were different, we have taken the average for these two sites in the minimization. We have a total of 196 spectral densities to derive ten global parameters. We found $Q=1.0\%$, and the calculated spectral densities are also shown in Figs. 4 and 5 as curves. Although there exist some systematic deviations between experimental and calculated spectral densities, the overall fits are quite satisfactory given the many simplifications (in particular the use of the ''pentane'' effect) in the motional model used in the present study. In Fig. 6 we present the site dependences of spectral densities at 378 K, and note the agreement between calculated and experimental values is quite good. We have also indicated in the same figure the ODF contributions $J_{1DF}^{(i)}(\omega)$ at 378 K.

All model parameters are summarized as plots shown in Fig. 7. The three-bond motions are found to be very fast as in other liquid crystals including 8OCB [17], and occur on a time scale of femtoseconds. Both k_2 and k_3 decrease with increasing temperature, while k_1 shows an opposite temperature behavior. Indeed, k_1 could also be approximated by an Arrhenius relation. Similar temperature dependences for k_1 and k_2 were observed in 6OCB [14] and 8OCB [17]. The activation energy $E_a^\parallel(=52.8$ kJ/mol) is higher than the activation energy $E_a^\perp(=26.7$ kJ/mol), which seems unphysical. This merely reflects the difficulty in obtaining information about the tumbling motion of the molecule, a phenomenon often encountered in NMR studies of liquid crystals [4,50,51]. We note that the $D_\parallel/D_\perp$ is of the order of 100 in the N_{re} phase of 8OBCB, which is consistent with that found in the N phase of 8OCB. The error limits for $E_a^\parallel$ lie between 51.8 and 53.7 kJ/mol, and those for $E_a^\perp$ lie between 25.7 and 27.6 kJ/mol. The error limit for a particular global parameter was estimated by varying the one under consideration while keeping all other global parameters identical to those for the minimum F, to give an approximate doubling in the F value. The pre-exponentials in Eqs. (11) and (12) are $D_\perp^\circ=5.83\times10^{11}$ s^{-1} and $D_\parallel^\circ=1.76\times10^{17}$ s^{-1}. When comparing these with those found in 8OCB, they are about three orders of magnitude smaller. This is understood by the difference in their temperature ranges, and not by the specific nature of the mesophases. The error limits for $D_\perp^\circ$ lie between 4.45×10^{11} s^{-1} and 8.15×10^{11} s^{-1}, and those for $D_\parallel^\circ$ between 1.35×10^{17} s^{-1} and 2.4×10^{17} s^{-1}. In estimating the error limits for jump rates, we examine their values at T_{max}: $k_1'=3.2\times10^{15}$ s^{-1}, $k_2'=5\times10^{11}$ s^{-1}, and $k_3'=2.4\times10^{17}$ s^{-1}.

We found that any larger k_3' or k_1' value does not affect the fits, and hence no upper limit can be estimated, while their lower limits are $k_1' = 2.54 \times 10^{15}$ s^{-1} and $k_3' = 3 \times 10^{15}$ s^{-1}. Indeed, there is a tendency in the minimization to overestimate the k_3 (or k_1) value. Now 4.0×10^{10} s$^{-1} < k_2' < 2.14 \times 10^{12}$ s^{-1}. We note that the lower limit for k_2' is for a 50% increase in F only, since this lower limit has less sensitivity in the fits. Finally, the correlation coefficients among various model parameters are addressed. The correlation coefficients between diffusion pre-exponentials and their corresponding activation energies are very high (near 1). Those for the pairs $(D_{\parallel}^{\circ}, D_{\perp}^{\circ})$, $(D_{\parallel}^{\circ}, E_a^{D_{\perp}})$, and $(D_{\perp}^{\circ}, E_a^{D_{\parallel}})$ are equal to 0.69, while for (k_1', k_1''), (k_2', k_2''), and (k_3', k_3'') are 0.98, 0.79, and 0.3, respectively. The correlation coefficients between one of the jump parameters in Eq. (13) with one of the diffusive parameters in Eqs. (11) and (12) are between 0.37 and 0.74, while those for the remaining pairs of jump parameters range between 0.07 and 0.9, e.g., (k_1', k_3''), (k_1', k_2''), and (k_2', k_3'') are 0.07, 0.9, and 0.5, respectively. The correlation coefficients involving the prefactor A are also estimated. For example, those for (A, ω_c), $(A, D_{\perp}^{\circ})$, $(A, E_a^{D_{\parallel}})$, and (A, k_3') are 0.97, 0.86, 0.47, and 0.29, respectively.

In conclusion, a consistent picture has emerged in interpreting the quadrupolar splittings and relaxation data in the N_{re} phase of 8OBCB. It is found that like the relaxation data in the N and S_A phases of 8OCB, the decoupled model can describe the correlated internal dynamics of the octyloxy chain, while the Nordio model can describe the overall motions. Also like the N phase of 8OCB, ODF contributions are needed to account for part of the spin relaxation in the N_{re} phase of 8OBCB. We believe that this observation simply reflects the differences in the viscoelastic coefficients due to the temperature range of N_{re} in 8OBCB. Indeed, we found that in the binary mixtures of 8OCB-d_{17}/6OCB [52] or 6OCB-d_{21}/8OCB [14] ODF were not required to explain the measured spectral densities in its low temperature N_{re} phase. Finally, the jump rate constants and the rotational diffusion constants are consistent with values found in other cyanobiphenyl compounds. However, the k_3 values found thus far for the crankshaft motion in several different liquid crystals seem a bit high, since this motion should involve relatively high activation energy even though the change in the overall molecular shape is small. Perhaps other types of motions which can induce transitions among allowable conformations should be considered in our rather simplified model. For instance, the type II motion of Skolnick and Helfand [53], which involves either a gauche migration or gauche pair formation in the chain, may be incorporated in our decoupled model instead of the k_3 motion (the so called type I motion by Skolnick and Helfand). This certainly requires further investigations, and is being pursued in our laboratory.

ACKNOWLEDGMENTS

We wish to thank Fundação para a Ciência e Tecnologia (FCT) through Project Nos. PBIC/C/CTM/1935/95, and the Natural Sciences and Engineering Council of Canada. A.C. thanks FCT for Grant No. PRAXIS XXI BD/2900/94. We also wish to acknowledge the contribution of Dr. G. M. Richards in the initial stage of this project.

[1] R. Y. Dong, *Nuclear Magnetic Resonance of Liquid Crystals* (Springer-Verlag, New York 1997).
[2] F. Noack, M. Notter, and W. Weiß, Liq. Cryst. **3**, 907 (1988).
[3] F. Noack and K. H. Schweikert, in *The Molecular Dynamics of Liquid Crystals*, edited by G. R. Luckhurst and C. A. Veracini (Kluwer, Dordrecht, 1994).
[4] J. M. Goetz, G. L. Hoatson, and R. L. Vold, J. Chem. Phys. **97**, 1306 (1992).
[5] R. Y. Dong, J. Chem. Phys. **75**, 2621 (1981).
[6] R. Y. Dong, Mol. Cryst. Liq. Cryst. Lett. **64**, 205 (1981).
[7] R. Y. Dong, J. Chem. Phys. **76**, 5659 (1982).
[8] R. Y. Dong, J. S. Lewis, E. Tomchuk, and E. Bock, Mol. Cryst. Liq. Cryst. **122**, 35 (1985).
[9] R. Y. Dong, G. M. Richards, J. S. Lewis, and E. Tomchuk, Mol. Cryst. Liq. Cryst. **144**, 33 (1987).
[10] K. H. Schweikert and F. Noack, Z. Naturforsch., A: Phys. Sci. **44**, 597 (1989).
[11] S. Miyajima, K. Akaba, and T. Chiba, Solid State Commun. **49**, 675 (1984).
[12] S. Miyajima and T. Chiba, J. Phys. Soc. Jpn. **57**, 2550 (1988).
[13] P. J. Sebastião, A. C. Ribeiro, H. T. Nguyen, and F. Noack, J. Phys. II **5**, 1707 (1995).
[14] X. Shen and R. Y. Dong, J. Chem. Phys. **108**, 9177 (1998).
[15] F. Noack, in *NMR Basic Principles and Progress*, edited by P. Diehl, E. Fluck, and R. Kosfeld (Springer-Verlag Berlin, 1971), Vol. 3, p. 84.
[16] F. Noack, in *Progress in NMR Spectroscopy* (Elsevier, Amsterdam, 1986), Vol. 18, p. 171.
[17] R. Y. Dong, Phys. Rev. E **60**, 5631 (1999).
[18] P. J. Sebastião, A. C. Ribeiro, H. T. Nguyen, and F. Noack, Z. Naturforsch., A: Phys. Sci. **48**, 851 (1993).
[19] R. Y. Dong and X. Shen, J. Phys. Chem. A **101**, 4673 (1997).
[20] R. L. Vold, R. R. Vold, and M. Warner, J. Chem. Soc., Faraday Trans. **84**, 997 (1988).
[21] G. van der Zwan and L. Plomp, Liq. Cryst. **4**, 133 (1989).
[22] T. Lubensky, Phys. Rev. A **2**, 2497 (1970).
[23] P. Pincus, Solid State Commun. **7**, 415 (1969).
[24] S. Miyajima and T. Hosokawa, Phys. Rev. B **52**, 4060 (1995).
[25] J. S. Lewis, E. Tomchuk, and E. Bock, Can. J. Phys. **69**, 1454 (1991).
[26] D. Imbardelli, B. Wazynska, A. Golemme, G. Chidichimo, and R. Dabrowski, Mol. Phys. **79**, 1275 (1993).
[27] F. Hardouin, A. M. Levelut, H. T. Nguyen, and S. Sigaud, Mol. Cryst. Liq. Cryst. Lett. **56**, 35 (1979).
[28] J. L. Figueirinhas, C. Cruz, A. C. Ribeiro, and H. T. Nguyen, Mol. Cryst. Liq. Cryst. **212**, 263 (1992).
[29] R. Tarroni and C. Zannoni, J. Chem. Phys. **95**, 4550 (1991).
[30] P. L. Nordio and P. Busolin, J. Chem. Phys. **55**, 5485 (1971); P. L. Nordio, G. Rigatti, and U. Segre, Mol. Phys. **25**, 129 (1973).
[31] J. M. Bernassau, E. P. Black, and D. M. Grant, J. Chem. Phys. **76**, 253 (1982).
[32] J. Bulthuis and L. Plomp, J. Phys. (Paris) **51**, 2581 (1990).
[33] E. Berggren, R. Tarroni, and C. Zannoni, J. Chem. Phys. **99**, 6180 (1993).

[34] E. Berggren and C. Zannoni, Mol. Phys. **85**, 299 (1995).
[35] A. Ferrarini, G. J. Moro, and P. L. Nordio, Liq. Cryst. **8**, 593 (1990).
[36] R. Y. Dong and G. M. Richards, Chem. Phys. Lett. **171**, 389 (1990).
[37] R. Y. Dong, Phys. Rev. A **43**, 4310 (1991).
[38] P. J. Flory, *Statistical Mechanics of Chain Molecules* (Wiley, New York, 1969).
[39] R. Y. Dong, Mol. Phys. **88**, 979 (1996).
[40] J. W. Emsley, G. R. Luckhurst, and C. P. Stockley, Proc. R. Soc. London, Ser. A **381**, 117 (1982).
[41] C. J. R. Counsell, Ph.D. thesis, Southampton University, Southampton, 1983; C. J. R. Counsell, J. W. Emsley, G. R. Luckhurst, and H. S. Sachdev, Mol. Phys. **63**, 33 (1988).
[42] C. J. R. Counsell, J. W. Emsley, N. J. Heaton, and G. R. Luckhurst, Mol. Phys. **54**, 847 (1985).
[43] J. P. Jacobsen, H. K. Bildsoe, and K. Schumburg, J. Magn. Reson. **23**, 153 (1976); S. B. Ahmad, K. J. Packer, and J. M. Ramsden, Mol. Phys. **33**, 857 (1977); R. R. Vold and R. L. Vold, J. Chem. Phys. **66**, 4018 (1977).
[44] R. J. Wittebort and A. Szabo, J. Chem. Phys. **69**, 1722 (1978).
[45] J. H. Freed, J. Chem. Phys. **66**, 4183 (1977).
[46] E. A. Joghems and G. van der Zwan, J. Phys. II **6**, 845 (1996).
[47] S. Wimperis, J. Magn. Reson. **83**, 590 (1990); **86**, 46 (1989).
[48] R. Y. Dong and G. M. Richards, J. Chem. Soc. Faraday Trans. **84**, 1053 (1988).
[49] W. H. Press, B. P. Flannery, S. A. Teukolsky, and W. T. Vetterling, *Numerical Recipes* (Cambridge University Press, Cambridge, 1986).
[50] R. Y. Dong and G. M. Richards, J. Chem. Soc., Faraday Trans. **88**, 1885 (1992).
[51] V. Rutar, M. Vilfan, R. Blinc, and E. Bock, Mol. Phys. **35**, 721 (1978).
[52] R. Y. Dong and M. Cheng, J. Chem. Phys. (to be published).
[53] J. Skolnick and E. Helfand, J. Chem. Phys. **72**, 5489 (1980).